



Deposited via The University of Leeds.

White Rose Research Online URL for this paper:

<https://eprints.whiterose.ac.uk/id/eprint/90216/>

Version: Accepted Version

Article:

Khuphe, M, Mukonoweshuro, B, Kazlauciusas, A et al. (2015) A Vegetable Oil-Based Organogel for use in pH-Mediated Drug Delivery. *Soft Matter*, 11. 9160 - 9167. ISSN: 1744-683X

<https://doi.org/10.1039/C5SM02176F>

Reuse

Items deposited in White Rose Research Online are protected by copyright, with all rights reserved unless indicated otherwise. They may be downloaded and/or printed for private study, or other acts as permitted by national copyright laws. The publisher or other rights holders may allow further reproduction and re-use of the full text version. This is indicated by the licence information on the White Rose Research Online record for the item.

Takedown

If you consider content in White Rose Research Online to be in breach of UK law, please notify us by emailing eprints@whiterose.ac.uk including the URL of the record and the reason for the withdrawal request.



A Vegetable Oil-Based Organogel for use in pH-Mediated Drug Delivery †

Mthulisi Khuphe,^a Blessing Mukonoweshuro,^b Algy Kazlaucinas^a and Paul D. Thornton*^a

Received 00th January 20xx,
Accepted 00th January 20xx

DOI: 10.1039/x0xx00000x

www.rsc.org/

Organogels prepared with vegetable oils as the liquid organic phase present an excellent platform for the controlled delivery of hydrophobic guest molecules. We disclose a graft copolymer comprised of a poly(L-serine) backbone linked to alkane side-chains by hydrolytically susceptible ester bonds, that is capable of gelating edible safflower oil. The thermoresponsive organogel formed, which is non-cytotoxic, is capable of withholding guest molecules before undergoing targeted disassembly upon incubation in solutions of acidic pH, permitting the directed release of payload molecules. The presented material offers an extremely promising candidate for the controlled delivery of hydrophobic agents within acidic environments, such as cancer tumour sites.

Introduction

Organogels are semi-solid materials in which an organic liquid forms a continuous phase that is immobilised within an extensive three-dimensional entwinement of gelator molecules (usually ≤ 5 wt.%).¹ Physical organogels entrap solvent molecules within a vast mesh fashioned by non-covalent interactions between polymer chains, ensuring that such gels are thermally reversible.² This (macro)molecular feature may readily be utilised for the entrapment and thermally-mediated release of substantial quantities of covalently unbound payload molecules.³

Despite these advantageous material qualities, the application of organogels as vehicles for controlled drug delivery has been hindered somewhat due to the cytotoxicity that is associated with numerous organic solvents. Many organogels have been reported that are formed using solvents including acetone,⁴ tetrahydrofuran (THF),⁵ toluene,⁶ chloroform,⁷ hexane,⁸ benzene,⁹ methanol,¹⁰ dichloromethane,¹¹ acetonitrile¹² and dimethylformamide (DMF),¹³ amongst others. Such solvents are either irritants, carcinogens, mutagens, teratogens or acute toxicants. Consequently, organogels have more commonly been employed within the non-biological settings of oil spill clean-up,¹⁴ dye spill clean-up,¹⁵ sensing devices¹⁶ and fuel cells for energy harvesting.¹⁷

Vegetable oils offer an alternative to conventional organic solvents for use as the continuous phase and may permit the creation of non-cytotoxic organogels suitable for application *in vivo*. Examples of vegetable oil-based organogels include organic gelators dispersed within sunflower oil,¹⁸ safflower oil¹⁹ and linseed oil.²⁰ Barbut and co-workers demonstrated an ethylcellulose-canola oil organogel as a potential replacement for the animal fat in frankfurters.²¹ Marangoni and co-workers also demonstrated the

use of canola oil as the solvent in 12-hydroxystearic acid-containing organogels that displayed tuneable crystallinity and oil binding capacity, depending on their storage temperature.²² The use of organogels as biomaterials is more limited. Noteworthy work by Leroux and co-workers demonstrated the formation of a number of alanine methyl ester-terminated fatty acid organogelators.²³ It was shown that N-lauroyl-L-alanine and N-lauroyl-L-alanine methyl ester could independently gelate soybean oil for the controlled release of dextran molecules.²⁴ Additionally, biocompatible N-Stearoyl-L-alanine methyl ester organogels formed in the presence of safflower oil showed promise for the controlled delivery of rivastigmine.²⁵ In addition, Lukyanova *et al.* reported the formation of an organogel consisting of 12-hydroxystearic acid as the gelator within non-toxic soybean oil.²⁶ The organogel formed, which was susceptible to degradation by lipase enzymes, was able to support the attachment and proliferation of Chinese hamster ovary fibroblast cells, highlighting the potential that the material possesses for application as a scaffold for tissue engineering. Finally, Work by Kakemi and co-workers demonstrated the use of 12-hydroxystearic acid-soybean oil organogels for the delivery of lipophilic²⁷ and hydrophilic²⁸ drug molecules. Lipase-mediated organogel degradation resulted in payload release, which was also demonstrated *in vivo*.

It is imperative that biomaterials intended to be applied *in vivo* as drug delivery vehicles are both biocompatible and can undergo programmed biodegradation.²⁹ Poly(amino acid)s are a class of macromolecule that offer both traits, and may be synthesised in a highly-controlled manner by N-carboxyanhydride ring-opening polymerisation (NCA ROP) reactions.³⁰ In addition, amino acids offer an extensive array of functional groups, including carboxylic acid, amine, thiol and hydroxyl groups that translate to the corresponding polymer.³¹ This enables the facile post-polymerisation functionalisation of poly(amino acid)s with groups that facilitate their hierarchical self-assembly into precisely defined nano and microstructures that may be exploited for use as drug delivery vehicles.³²

Organogels formed from poly(amino acid) gelators dispersed in vegetable oils have the potential to be an extremely effective class

^a School of Chemistry, University of Leeds, Leeds, LS2 9JT, United Kingdom. Email: p.d.thornton@leeds.ac.uk. Tel: +44 (0)113 3432935.

^b Institute of Medical & Biological Engineering, University of Leeds, Leeds, LS2 9JT United Kingdom.

†Electronic Supplementary Information (ESI) available: Full material characterisation including: ¹H NMR spectra, TGA, DSC and UV/Vis spectrophotometry data. See DOI: 10.1039/x0xx00000x

of drug delivery vehicle. If designed and synthesised correctly, such materials offer biocompatibility and biodegradability, in addition to being created from renewable sources. In this paper, we describe the synthesis and characterisation of a novel organogel formed from a poly(amino acid)-containing polymer that is dispersed within edible safflower oil. A graft copolymer consisting of a poly(serine) (PS) backbone conjugated with pendant octadecanoic acid branches acts as a biodegradable gelator, that is susceptible to hydrolysis under acidic conditions. The organogel formed is thermoresponsive and possesses the capability to encapsulate a molecular cargo, before undergoing acid-induced degradation and consequent payload release. The material generated is an excellent candidate as an injectable drug carrier vehicle for the controlled delivery of non-polar therapeutic agents within acidic environments, such as cancerous tissue.³³

Experimental Section

Materials and Methods

Triphosgene (98%), anhydrous ethyl acetate (99.8%), anhydrous THF ($\geq 99.9\%$), n-hexane (98%), anhydrous DMF (99.8%), diethyl ether (99.8%), benzylamine (99%) and O-Benzyl-L-serine (99%) were all acquired from Sigma Aldrich. α -Pinene (98%) and phosphate buffered saline (PBS) buffer (Dulbecco 'A' tablets) were supplied by Thermo Fisher Scientific Laboratories. Rhodamine B (98%) was supplied by Alfa Aesar. HPLC grade water (18.2 M Ω .cm) was supplied by VWR International. All chemicals were used as received unless stated otherwise.

¹H NMR spectra were recorded at 500 MHz on a Bruker Avance 500 spectrometer, in DMSO-d₆ for the NCA monomer and in trifluoroacetic acid-d for the polymers produced, at 25 °C. ¹H NMR spectra were analysed using MestreNova® Research Lab software. Electrospray Ionisation Mass spectrometry (ESI-MS) was performed using a Thermo Scientific Ultimate 3000 mass spectrometer. Elemental analysis was conducted using a Thermo FlashEA Analyzer, 1112 Series. FTIR measurements were performed using a Bruker Alpha-P spectrometer, equipped with a diamond ATR crystal. Rheological tests were carried out at 37 °C using a stress-controlled AR 1500ex rheometer (TA Instruments). The instrument was equipped with a steel-parallel plate geometry (40 mm in diameter) with the geometry gap distance maintained at 500 μ m. The linear viscoelastic region (LVER) of the gel sample was determined by conducting a stress sweep test at a constant frequency (6.28 rad.s⁻¹). The storage modulus (G') and the loss modulus (G'') were determined by performing a frequency sweep test (0.1 rad.s⁻¹ to 628 rad.s⁻¹) at a constant stress (5 Pa). Scanning electron microscopy (SEM) was performed using a JEOL JSM-6610LV microscope (Oxford Instruments) equipped with a field emission electron gun as an electron source, using a working distance of 11 mm. An accelerating voltage of 15 kV was applied. Differential scanning calorimetry (DSC) was carried out using a DSC Q20 unit (TA instruments) calibrated with indium. A TGA Auto Q20 unit (TA Instruments) was used for thermogravimetric analysis (TGA).

Synthesis of the NCA of O-benzyl-L-serine

A well-reported literature procedure was followed for the synthesis of the NCA of O-Benzyl-L-serine.³⁴ Yield: 4.98 g, 22.5 mmol, 88 %. Melting range: 99 °C - 100 °C. ¹H NMR (500 MHz, DMSO, δ , ppm): 9.12 (s, 1H, NH), 7.39 - 7.29 (m, 5H, ArH, J = 50 Hz), 4.68 - 4.67 (t, 1H, α CH, J = 5 Hz), 4.58 - 4.52 (q, 2H, CH₂, J = 30 Hz), 3.79 - 3.63 (m, 2H, CH₂, J = 80 Hz). ESI MS (244 m/z, M⁺ Na⁺).

Synthesis of Poly(O-benzyl-L-serine)

The NCA of O-benzyl-L-serine (0.825 g, 3.74 mmol) was dissolved in anhydrous DMF (20 mL) in a nitrogen-purged Schlenk tube equipped with a magnetic stirrer bar. To this, a solution of benzylamine (20 mg, 0.187 mmol) in anhydrous DMF (10 mL) was added. The reaction was allowed to stir at room temperature for 96 hours under an inert nitrogen atmosphere. The polymer was precipitated in diethyl ether and isolated by centrifugation (6000 rpm, 15 min, 5 °C). The recovered polymer was washed three times using cold diethyl ether and subsequently dried in a vacuum oven (40 °C) for 48 hours. Yield: 422.6 mg, 62 wt.%. ¹H NMR (500 MHz, TFA-d, ppm): 7.45 - 7.30 (107 H, ArH), 5.04 - 4.81 (19 H, α CH), 4.81 - 4.49 (40 H, ArCH₂), 4.35 - 3.79 (40 H, CH₂O).

Deprotection of Poly(O-benzyl-L-serine)

Poly(O-benzyl-L-serine) (350 mg) was weighed into a 50 mL round bottom flask equipped with a magnetic stirrer bar. TFA (7 mL) was added to dissolve the polymer. 3 mL of HBr solution in acetic acid (33 wt.%) was added and the solution was left to stir at room temperature for 16 hours. The deprotected polymer was precipitated into diethyl ether (100 mL) and isolated by centrifugation. The recovered polymer was washed three times using cold diethyl ether and subsequently dried in a vacuum oven (40 °C) for 48 hours. Yield: 87 wt. %. GPC (DMF + LiBr): M_n = 1862, M_w = 1959, PDI = 1.05. ¹H NMR (500 MHz, TFA-d, ppm): 7.45 - 7.30 (6H, ArH), 5.04 - 3.79 (61 H, COCH(NH)CH₂OH). ESI MS in DMSO (1847 Da, M⁺ H⁺).

Synthesis of Poly(serine)-g-octadecanoic acid (PSSA)

Octadecanoic acid (1.54 g, 5.41 mmol) was dissolved in anhydrous DMF (10 mL). The solution was injected into a 100 mL round bottom flask sealed with a rubber septum and nitrogen-purged. Poly(L-serine) (PS) (250 mg, 0.134 mmol) was dissolved in anhydrous DMF by sonication for 3 hours and then added to the Schlenk tube. 4-dimethylaminopyridine (DMAP) (33.1 mg, 0.271 mmol) was dissolved in anhydrous DMF (10 mL) and also added to the Schlenk tube. The reaction was cooled to 0 °C. Dicyclohexylcarbodiimide (DCC) (0.670 g, 3.25 mmol) was dissolved in anhydrous DMF (10 mL) and then added drop-wise to the cooled reaction mixture over 15 minutes. The reaction was stirred at 0 °C for a further 30 minutes and then left at room temperature for 48 hours, after which the precipitated dicyclohexylurea (DCU) was isolated. The reaction mass was stored overnight at -5 °C and any precipitated DCU was isolated. The supernatant was added drop-wise to cold diethyl ether (500 mL) to precipitate the polymeric product. The obtained product was isolated by centrifugation (6000 rpm, 20 min, -10 °C), washed several times with cold ether and dialysed against distilled water for 72 hours. The polymer was then recovered by lyophilisation. Yield: 77.3 wt. %. ¹H NMR (500 MHz, TFA-d, ppm): 8.53 (8H, NH), 7.45 - 7.30 (6H, ArH), 5.04 - 3.79 (60H, COCH(NH)CH₂OH), 2.22 - 2.64 (13H, CH₂)₂COO), 1.53 - 1.41 (37H, (CH₂)₁₄), 0.99 - 0.97 (4H, CH₃).

Preparation of Xerogels for SEM Analysis

A method previously reported by Rogers *et al* was adopted to form xerogels from the PSSA-safflower oil organogels, that were suitable for analysis by SEM.³⁵ Xerogels were obtained by extracting the oil from the gel matrix using an n-hexane/acetone cocktail (8:2 v/v), over a period of 24 hours. The obtained xerogels were then deposited carefully onto SEM glass cover slides mounted on SEM stubs using conducting tap and then allowed to air-dry prior to sputter-coating with a thin layer of gold.

Coating of Cell culture Wells

The 2% wt organogel was prepared by dissolving PSSA (36.5 mg) in safflower oil at 50 °C (1.79 g). A 50 $\mu\text{g}\cdot\text{mL}^{-1}$ solution of type 1 rat tail collagen was prepared in PBS, pH-adjusted to pH 7 and then autoclaved. Briefly, two sets of triplicate wells per 96-well microplate were coated at their base with PSSA-safflower oil organogel (30 μL per well), rat tail collagen (30 μL per well) or left uncoated (i.e. Nunclon Δ^{TM} surface). Furthermore, one more set of triplicate wells was coated with cyanoacrylate ('super glue') (30 μL per well). Prior to coating with the gel, the gel was reheated into solution and then in situ gelation was allowed for the solution deposited in the wells. All the coated microplates were incubated for 3 hours at room temperature in a class II biohazard cabinet prior to use.

Cell Seeding

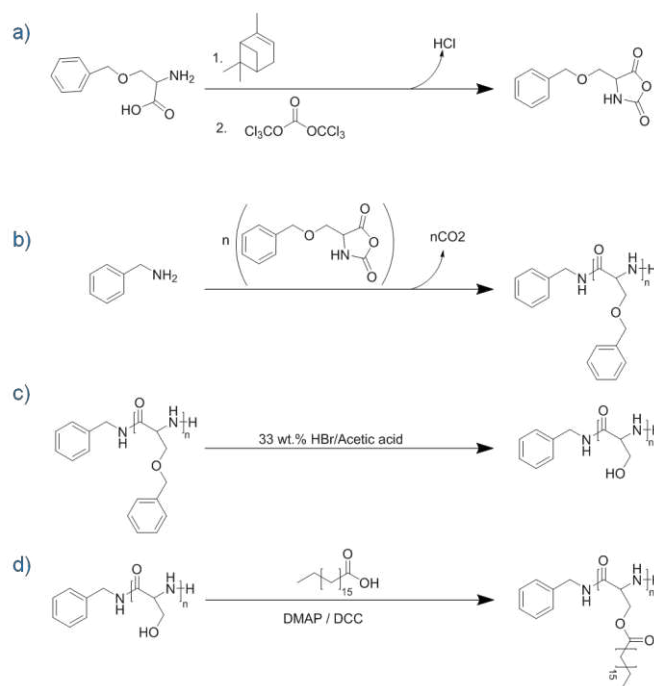
Triplicate wells coated with PSSA-safflower oil organogel, type 1 rat tail collagen, Nunclon Δ^{TM} surface and cyanoacrylate were seeded with 5×10^4 C3H mouse dermal fibroblasts, respectively (Fig. S8, ESI †). Dulbecco's Modified Eagle Medium (DMEM) supplemented with a 10 % (v/v) foetal bovine serum (FBS), L-glutamine (1 mM) and penicillin (100 U. mL^{-1}) and streptomycin (100 $\mu\text{g}\cdot\text{mL}^{-1}$) cocktail was then added to bring the total volume in each well to 200 μL . In another set of triplicate wells coated with the PSSA-safflower oil organogel, type 1 rat tail collagen and Nunclon Δ^{TM} surface, no cells were seeded but the wells were filled with DMEM (200 μL). Empty peripheral wells were filled with sterilised PBS so as to keep the environment humid and reduce the evaporation from the seeded wells. The seeded microplates (x3) were incubated in a humidified incubator at 37 °C and 5 % (v/v) CO_2 in air for 24 hours, 72 hours and 120 hours.

ATPlite-M $^{\text{®}}$ Assay

The viability of the previously seeded mouse dermal fibroblasts was assessed at 24 hour, 72 hour and 120 hour time intervals. 100 μL of culture medium was pipetted out of the respective wells and replaced with mammalian cell lysis solution (50 μL). The microplate was agitated at room temperature (700 rpm, 5 minutes) on an orbital microplate shaker. Lysed contents of the wells were then transferred to a white 96-well ViewPlate microplate and reconstituted substrate solution (50 μL) was added. The microplate was sealed to prevent contamination, shielded from light by wrapping in an aluminium foil and agitated (700 rpm, 5 minutes) at room temperature. Bubbles formed during agitation were removed quickly by flaming and the microplate was re-sealed and dark-adapted inside the plate reader for 10 minutes. Luminescence counting was then carried out on a Hidex Chameleon plate reader equipped with Mikrowin 2000 software from Mikrotek Laborsysteme GmbH.

Results and discussion

A polymer gelator was synthesised that was envisaged to possess the capability to form hydrogen bonds between adjacent poly(amino acid) backbone chains,³⁶ and form hydrophobic interactions between adjacent, grafted, alkyl chains,³⁷ to facilitate organogel formation. Initially, poly(O-benzyl-L-serine)₂₀ was synthesised by the ROP of O-benzyl-L-serine NCA, using benzylamine as the initiator, before the benzyl ether protecting group was cleaved from the polymer to yield PS (Scheme 1), as confirmed by ^1H NMR spectroscopy (Fig. S2, ESI †) and FTIR (Fig. 1a). The former



Scheme 1: The synthetic route to the PSSA gelator. Synthesis of the NCA of O-benzyl-L-serine (a), synthesis of poly(O-benzyl-L-serine) by NCA ROP (b), the creation of PS (c) and then PSSA (d).

displayed a reduction in the integral values corresponding to aromatic protons, with the peaks remaining calculated to be the aromatic protons of the benzylamine initiator. FTIR revealed a reduction in the peaks corresponding to the aromatic C-H's out of plane bending (700 cm^{-1} - 900 cm^{-1}). The molecular weight of PS calculated from ^1H NMR was found to be 1773.1 $\text{g}\cdot\text{mol}^{-1}$ by comparing the integral of the aromatic protons of benzylamine (7.45 ppm - 7.30 ppm) to the integral of the α -protons (5.04 ppm - 4.81 ppm). A comparable value was found by GPC (1862 $\text{g}\cdot\text{mol}^{-1}$) (Fig. S3, ESI †) and ESI-MS (1847 $\text{g}\cdot\text{mol}^{-1}$), further suggesting total polymerisation, and complete removal of the benzyl ether protecting groups. ESI-MS revealed a fragmentation pattern that is characterised by an increment of 87 m/z , representative of the serine repeat unit (Fig. S4, ESI †). PSSA was then obtained by grafting octadecanoic acid to the hydroxyl groups of PS (Scheme 1d) by DCC-mediated esterification. The successful grafting of octadecanoic acid was confirmed by the presence of the CH_2 alkyl chain in the FTIR spectrum (Fig. 1a, *bottom*). ^1H NMR analysis revealed that alkyl grafting had occurred by displaying peaks that are characteristic of the alkyl chain of octadecanoic acid (0.97 ppm - 2.22 ppm, Fig. S5, ESI †). The DSC thermogram of octadecanoic acid (Fig. 1b, *top*) reveals an endotherm corresponding to the melting point (71.5 °C). This thermal transition is present in the thermogram of the derivatised polymer (Fig. 1b, *bottom*), but is absent from the thermogram of PS (Fig. 1b, *middle*), further confirming successful esterification. Finally, the successful grafting of alkyl chains was demonstrated by an increase in the overall carbon content from 36.5 % to 69.4 % when PS was converted to PSSA, as determined by elemental analysis. This was accompanied by an increase in the overall hydrogen content and a decrease in the nitrogen content (Table S2, ESI †). By comparing the overall carbon content of PSSA to the theoretical carbon content that equates to complete PS modification, it can be concluded that, the grafting efficiency is 97.3%.

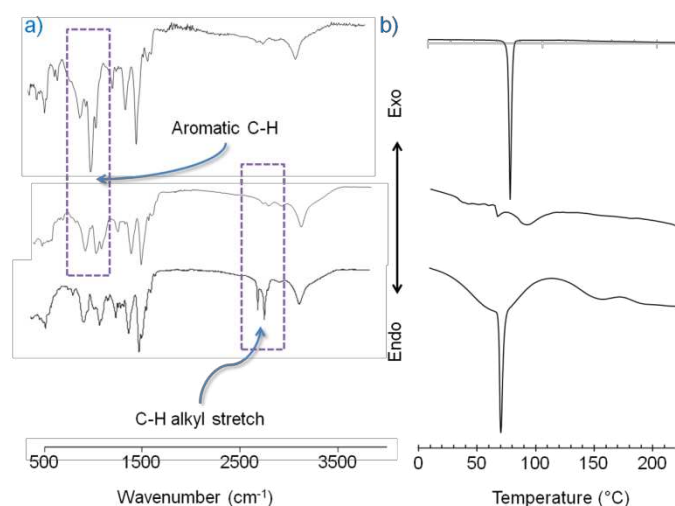


Fig. 1: a) FTIR spectra of poly(O-benzyl-L-serine), *top*, PS, *middle* and PSSA, *bottom*. b) Comparison of the DSC thermograms of octadecanoic acid, *top*, PS, *middle* and PSSA, *bottom*. The successful grafting of octadecanoic acid to PS is evidenced by the emergence of the melting point endotherm at 71.5 °C. on the thermogram of PSSA. (Endo = endotherm, Exo = exotherm).

The capability of PSSA to induce the gelation of safflower oil was assessed by heating the polymer in safflower oil to achieve dissolution. Gelation was observed upon cooling, due to the self-aggregation of the PSSA macromolecules (Fig. 2, *top*). PSSA was found to induce the gelation of safflower oil at polymer concentrations of 2 wt.% and greater. DSC was employed to analyse the thermal properties of this organogel using a heating cycle of between -20 °C and 80 °C as it is within the confines of the envisaged application temperatures. The thermogram produced displayed an endotherm that has a minimum point at 45.9 °C which is attributed to the gel/sol transition (Fig. S6, ESI†). This endothermic peak was present in numerous (at least six) heat-cool cycles, demonstrating the thermal reversibility that the material possesses. The broad nature of the peak indicates the aggregates are polydisperse.³⁸ The sol/gel transition was found to be represented by a maximum point at 37.2 °C in the cooling cycle (Fig. S7, ESI†). The temperature corresponding to gel/sol transition is higher than the one corresponding to sol/gel transition. This is a consequence of the hysteresis behaviour which is a common feature of thermoreversible organogels.³⁹

The morphology of the 2 wt.% organogel was assessed by imaging xerogels of the polymers formed by SEM. The microstructures formed possessed an interconnected porous 3D network (Fig. 2a) with pores typically of *ca* 1.5 μm in width, as observed at higher magnification (Fig. 2b). The porous nature of the organogels confirms their suitability for employment as a drug delivery carrier in which hydrophobic therapeutic agents may occupy the considerable voids present within the structure.

The thermal stability of the 2 wt.% organogel was determined by measuring its weight loss upon heating, by TGA. The organogel was found to be thermally stable when heated within the confines of the envisaged application temperatures, losing only 0.29 % of its original mass when heated to 80 °C (Fig. S8, ESI†).

Rheometry was employed to determine the mechanical properties of the organogels formed. Ideal gels behave as viscous flowing liquids over long time scales and so the storage modulus (G') must dominate the loss modulus (G'') in order for the system to be qualified as a gel.⁴⁰ Initially, the linear viscoelastic region

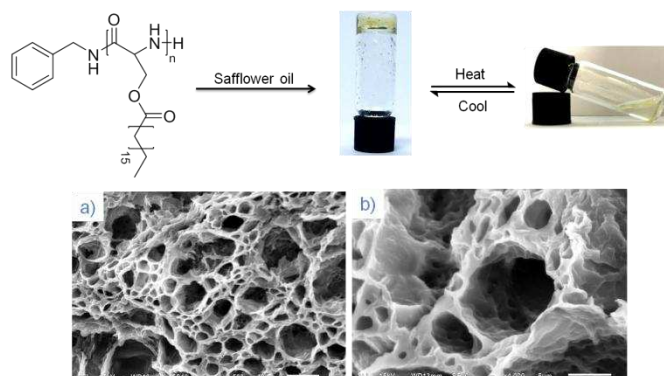


Fig. 2: *Top* PSSA (left) forms an organogel when dispersed in safflower oil (centre) that is thermoreversible (right). *Bottom* SEM micrographs showing the morphology of the 2 wt.% organogel. Scale bars represent a) 10 μm, b) 5 μm.

(LVER) of the 2 wt.% organogel was determined by performing an amplitude sweep at a constant angular frequency (6.28 rads^{-1}) (Fig. 3a). At low stress values, the elastic modulus dominates the loss modulus by almost one order of magnitude indicating a wholly elastic, intact organogel. Partial break-up of the organogel is evidenced by the drop in G' when the stress is gradually increased and structural failure is more pronounced at the yield stress (*ca* 35 Pa) where the gel begins to flow. A frequency sweep test (Fig 3b) was conducted within the limits of the LVER of the organogels and further confirmed that the system has an internal network. Furthermore, the moduli of the organogel (both G' and G'') do not exhibit a dependency on the applied frequency, which suggests that the organogel has a good tolerance for the external forces being exerted on it. The G' value of the organogel was observed to be $8.3 \times 10^3 \text{ Pa}$, which compares well with other organogels reported in the literature.⁴¹ The loss factor ($\tan \delta$) decreased slightly with an increase in frequency and remained below 1, indicating that the gel became more elastic and dissipated less energy (Fig. 3c).

To investigate material biocompatibility, and hence the suitability of using PSSA-safflower oil organogel as an injectable biomaterial, C3H mouse dermal fibroblasts were cultured in triplicate wells coated with the 2 wt.% PSSA-safflower oil organogel for 24, 72 and 120 hours. Cells cultured on super-glue (80-100 % (v/v) cyanoacrylate) and Nunclon Δ^{TM} -coated surfaces (tissue culture plastic) were used as controls for non-viable and viable cells respectively. Cells were also cultured in type I collagen-coated wells as a control. An ATP assay was employed to determine the biocompatibility of the organogels. ATP is present in all metabolically active cells and so the production of ATP can be used as a marker of cell viability and proliferation, whereby an increase in cellular ATP content over time is indicative of cell proliferation. The ATPlite-M[®] assay (Perkin Elmer) is based on chemiluminescence and affords a facile route to quantitatively measuring cellular ATP content. It utilises the reaction of ATP with the substrate D-luciferin in the presence of atmospheric oxygen to produce oxyluciferin, adenosine monophosphate, carbon dioxide, inorganic pyrophosphate and light. The light produced from this reaction is directly proportional to the cellular ATP content and can be detected easily using a luminescence counter.⁴²

The results obtained reveal that after 24 hours, the cellular ATP levels of the cells cultured on the organogel were not significantly different to those of cells cultured on collagen and the Nunclon Δ^{TM} surface, but were significantly different to those cultured on cyanoacrylate ($p < 0.05$, 2-way ANOVA) (Fig. 4). After 72 hours, the

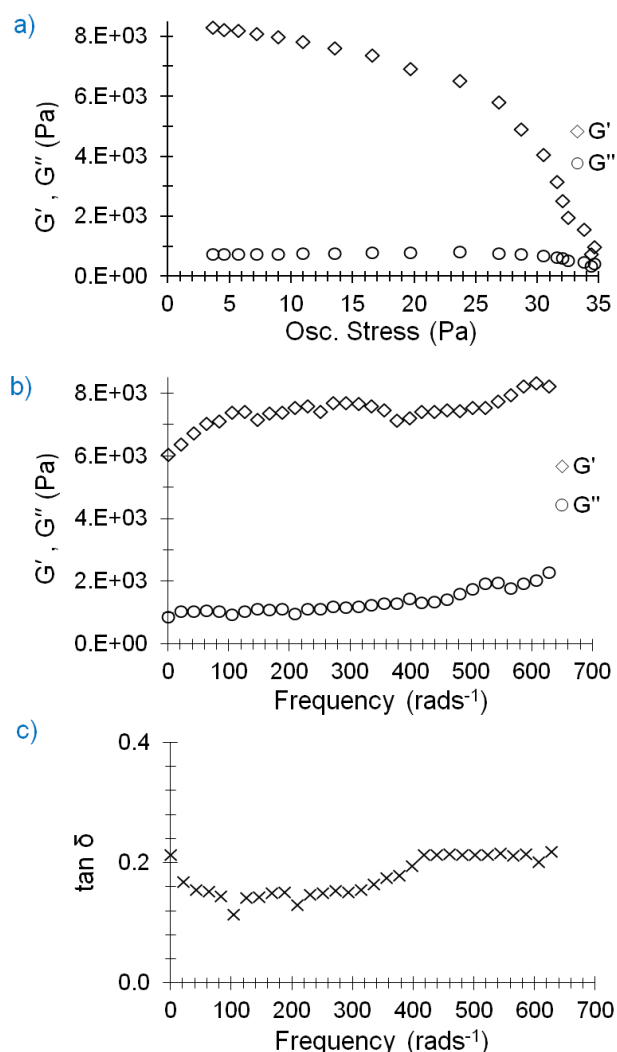


Fig. 3: Rheological analysis of the PSSA-safflower oil organogel a) amplitude sweep test, b) frequency sweep test and c) variation of the tangent of the phase angle (δ) with frequency.

ATP content of all the cells cultured on organogel, type I collagen and Nunclon Δ^{TM} -coated surfaces collagen and Nunclon increased markedly, and no significant difference in ATP levels was found between cells present on collagen and the organogels. The ATP levels of the cells seeded on the Nunclon Δ^{TM} surface was significantly greater than these two substrates however (3x higher than collagen and 4x higher than the organogel). Importantly, the ATP levels of the cells seeded on the organogel quadrupled between 24 and 72 hours. After 120 hours, there was no further increase in the ATP content of the cells cultured on the organogels, compared to 72 hours. For cells cultured on the Nunclon Δ^{TM} surface, there was a decline between 72 and 120 hours, although this was not significant. Conversely, there was a significant increase in the ATP content measured for the cells cultured on collagen between 72 hours and 120 hours. These findings demonstrate that the organogel presented is able to support cell adhesion, growth and proliferation, and is not cytotoxic. Although the ATP levels of the cells cultured on the organogel were lower compared to those cultured on the Nunclon Δ^{TM} surface, the trend was similar between these surfaces. The cells grown on the organogel increased their ATP level four-fold between 24 to 72 hours which is indicative of cell proliferation. Importantly, the ATP levels did not decline

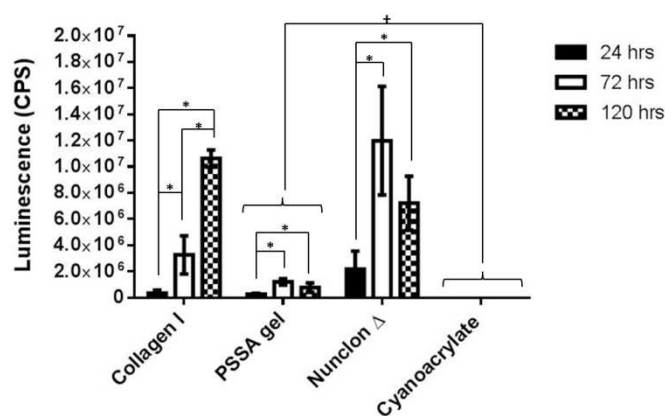


Fig. 4: Determination of the suitability of PSSA gel in supporting cell growth and proliferation. C3H mouse dermal fibroblasts (5×10^4) were seeded in triplicate wells pre-coated with PSSA the organogel, type 1 collagen (control for a biological substrate), Nunclon Δ^{TM} surface (tissue culture plastic control) and cyanoacrylate (cytotoxic surface control) for 24, 72 and 120 hours. Data was collected as counts per second using a Hidex Chameleon luminescence plate reader. Data ($n=3$) is presented as mean cps \pm 95 % CL following analysis by 2-way ANOVA ($p < 0.05$) and the Tukey method for computing the minimum significant difference (MSD) to determine individual differences between time points and surface coating. * represents significant differences between time points and + represents significant difference between PSSA-safflower oil gel and the cyanoacrylate surfaces. turned from pink (unseeded control) to yellow (seeded) after 120 hours which is indicative of cellular metabolism (Fig. S9, ESI †).

significantly between 72 hours and 120 hours, suggesting that the cells were viable and that the gel was not cytotoxic, unlike cyanoacrylate. The culture medium in the seeded coated wells (with the exception of cyanoacrylate) turned from pink (unseeded control) to yellow (seeded) after 120 hours which is indicative of cellular metabolism (Fig. S10, ESI †).

Acid-catalysed organogel degradation may be exploited as a trigger to release a therapeutic payload within acidic cancerous tissue. The pH values within the primary and secondary lysosomes of the cancer cells that form solid tumours has been reported to be as low as pH 4.⁴³ This acidic environment has been exploited for the intracellular release of drug molecules and fluorescent dyes from pH-sensitive polymeric carriers.⁴⁴ In addition, the acidic pH of vaginal fluid (pH 4.2) ensures that the reported organogels may be of significance for the delivery of antiviral therapies by vaginal administration.⁴⁵ Recent work conducted independently by Wu *et al.*⁴⁶ and Bunzen and Kolehmainen⁴⁷ demonstrated the targeted hydrolysis of imine links to cause organogels disassembly. We assessed the capability of organogels formed at 2 wt.% and 4 wt.% PSSA in safflower oil to release rhodamine B in response to cleavage of the ester bonds that link the graft copolymer by acid-catalysed hydrolysis. Rhodamine B was selected as a model payload due to its fluorescence insensitivity upon changes in solution pH results in polymer degradation, and organogel disruption.

The release of rhodamine B from the organogels created was found to be greatest when the organogel was incubated in acidic (pH 4.2) PBS buffer; in excess of 75% of total rhodamine B was released from the 2 wt.% gel after 78 hours (Fig. 5). On the contrary, release of rhodamine B from the organogel that was incubated at pH 7.4 was found to be negligible, with less than 5% of total rhodamine B being expelled over the 78 hour period. When

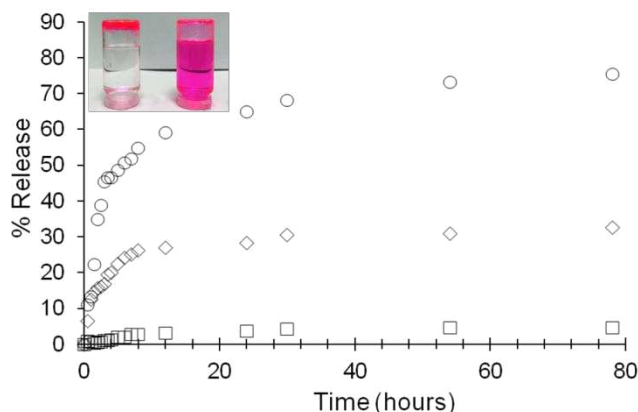


Fig. 5: The release of rhodamine B from a 2 wt.% PSSA-safflower oil organogel in response to incubation in PBS buffer maintained at pH 7.4 (\square) and pH 4.2 (\circ), and release from the 4 wt.% PSSA-safflower oil organogel at pH 4.2 (\diamond). The insert shows rhodamine B-loaded 2 wt.% PSSA-safflower oil organogel maintained within solution of pH 7.4 for 78 hours (left), and the remains of rhodamine B-loaded 2 wt.% PSSA-safflower oil organogel maintained within solution of pH 4.2 for 78 hours (right).

the PSSA content within the organogel was increased from 2 wt.% to 4 wt.%, and the release of rhodamine B was monitored at pH 4.2, the amount of rhodamine B released was found to be 32% over 78 hours, demonstrating that the modification of the organogels composition may be exploited to alter the payload release profile. Complete UV-Vis spectrophotometry data that details the release of rhodamine B from 2 wt.% organogels incubated at pH 4.2 and pH 7.4 is provided in Fig. S13, ESI[†].

The release mechanism of the encapsulated rhodamine B molecules was studied by fitting the experimental data to the Korsmeyer–Peppas (KP) model.⁴⁸ Using this model, which is represented by Equation 1, the release exponent (n) can be determined by statistical analysis. For $n \leq 0.45$, the release of the encapsulated cargo follows Fickian diffusion, in which polymer relaxation dominates the rate of diffusion of the encapsulated cargo. Deviation from Fickian diffusion occurs for values greater than 0.45, whereby the rate of diffusion of the encapsulated cargo and polymer relaxation are comparable. That is, for $0.45 < n < 0.89$ the release is considered to be non-Fickian (anomalous) which could be due to a variety of factors, including the surface erosion or bulk erosion of the delivery vehicle.

$$\frac{M_t}{M_\infty} = kt^n \quad (1)$$

Whereby, M_t and M_∞ represent the cumulative amount of drug released at time t and infinite time, respectively (hence, M_t/M_∞ is the fractional drug release at time t), n is the release exponent indicative of the release mechanism and k is the rate constant that takes into account the geometric characteristics of the organogel and the encapsulated cargo. Using Equation 2, generated by the differentiation of Equation 1, a linear plot can be obtained that has a slope which is the release exponent (n) and may be used to determine whether the release of rhodamine B followed a Fickian, or non-Fickian diffusion profile.

$$\log(\text{release } \%) = \log\left[\frac{M_t}{M_\infty}\right] = n \log t + \log k \quad (2)$$

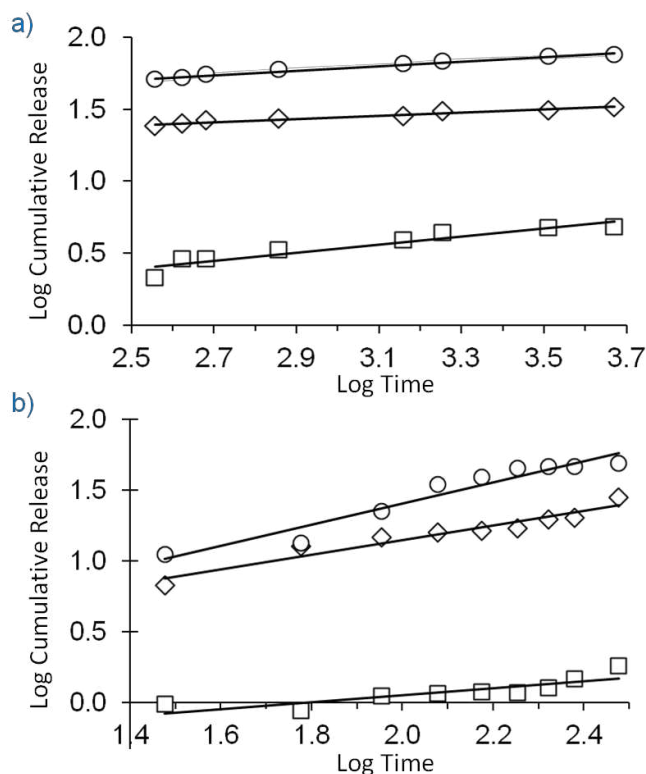


Fig. 6: KP model Plots for; 2 wt.% PSSA-safflower oil organogel incubated in PBS buffer maintained at pH 7.4 (\square) and at pH 4.2 (\circ), and a 4 wt.% PSSA-safflower oil organogel incubated in PBS buffer maintained at pH 4.2 (\diamond); from 0–5 hrs (a) and 6–78 hrs (b).

Fitting the experimental data to Equation 2 yields the linear plots of the logarithm of rhodamine B release (%) against the logarithm of time (Fig. 6). The gradient of each plot represents the release exponent at that time interval and pH (Table S3, ESI[†]). Analysis of the experimental data revealed that $0.45 < n < 0.89$ in the period ranging from 0 to 5 hours for the PSSA-safflower oil organogels incubated in the buffer maintained at pH 4.2. Specifically, the value of n was found to be 0.75 for the 2 wt.% organogel and 0.52 for the 4 wt.% organogel. According to the KP model, these values suggest that the release of the encapsulated rhodamine B is anomalous (non-Fickian) within this period. Surface erosion, driven by the acid hydrolysis of the organogel matrix is likely to be the dominant mechanism by which the dye is released. Increasing the loading of the gelator from 2 wt.% to 4 wt.% caused the delayed release of rhodamine B due to the accompanying increase in the crosslink density of the gel matrix. However, in the same time period, the release of rhodamine B from the 2 wt.% organogel incubated in PBS buffer maintained at pH 7.4 was found to follow Fickian diffusion ($n = 0.25$). This is expected as pH 7.4 solution cannot induce the degradation of the organogel matrix. This also supports the negligible release of rhodamine B at pH 7.4, in contrast to enhanced release from the organogels in pH 4.2 solution. On the contrary, the release of rhodamine B from the organogels between 6 and 78 hours of incubation was found to be slow and to follow a Fickian diffusion profile ($n < 0.45$), regardless of the solution pH. This could be due to the greater time required for the rhodamine B molecules to migrate from deep within the gel matrix to the release medium.

Macroscopic images obtained after 78 hours show that the encapsulated molecules are retained within the gel structure to a greater extent when maintained at pH 7.4 (Fig. 5, insert, left) compared to pH 4.2 (Fig. 5, insert, right), as indicated by the

breakdown of the organogel and consequent release of rhodamine B within the acidic solution. The residual weights of the organogels after 78 hours of incubation were measured and further demonstrate greater erosion of the 2 wt.% organogel that was incubated at pH 4.2 (ca 80 % weight lost) compared to the limited weight loss of the same class of organogels maintained in pH 7.4 solution (ca 14 % weight loss).

Conclusions

The hydroxyl groups of PS were utilised to graft octadecanoic acid to yield a macromolecule capable of gelating edible safflower oil. Organogels were formed at polymer concentrations of as low as 2 wt.% that were thermoreversible, offering the material great potential for use as an injectable biomaterial. Additionally, the organogel produced possessed considerable mechanical strength, with an elastic modulus of almost 10^4 Pa. The organogel was pH-responsive and could be eroded to release encapsulated rhodamine B when incubated at 37 °C in an acidic environment. Furthermore, the organogel possessed biocompatibility comparable to collagen and so offers a conducive environment for the growth and proliferation of mammalian cells. As such, the organogel detailed offers significant promise for use as an injectable carrier vehicle for the controlled delivery of therapeutic molecules to disease-infected cells, such as cancerous cells, that present an acidic environment *in vivo*.

Acknowledgements

The authors are extremely grateful to the Beit Trust and the University of Leeds for the financial support afforded to this work. We also thank Dr. Clare Mahon for conducting GPC analysis and Professor Eileen Ingham for providing assistance with biological analysis.

Notes and references

- (a) S. Mukherjee, C. Shang, X. Chen, X. Chang, K. Liu, C. Yu and Y. Fang, *Chem. Commun.* 2014, **50**, 13940; (b) R. Yang, S. Peng and T. C. Hughes, *Soft Matter*, 2014, **10**, 2188; (c) M-M. Su, H-K. Yang, L-J. Ren, P. Zheng and W. Wang, *Soft Matter*, 2015, **11**, 741.
- G. Yu, X. Yan, C. Han and F. Huang, *Chem. Soc. Revs.* 2013, **42**, 6697.
- A. Vintiloiu and J-C. Leroux, *J. Control. Release*, 2008, **125**, 179.
- M. Suzuki, Y. Nakajima, M. Yumoto, M. Kimura, H. Shirai, and K. Hanabusa, *Org. & Biomol. Chem.* 2004, **2**, 1155.
- T. Zhang and Q. Guo, *Chem. Commun.* 2013, **49**, 11803.
- H-K Yang, M-M Su, L-J Ren, P. Zheng and W. Wang, *RSC Adv.* 2014, **4**, 1138.
- C-B. Huang, L-J. Chen, J. Huang and L. Xu, *RSC Adv.* 2014, **4**, 19538.
- S. Kizil, K. Karadag, G. Ozan Aydin, H. J. Bulbul Sonmez, *J. of Environ. Man.* 2015, **149**, 57.
- S. Ghosh, R. Das Mahapatra and J. Dey, *Langmuir*, 2014, **30**, 1677.
- K.T. Kim, C. Park, G. W. M. Vandermeulen, D. A. Rider, C. Kim, M. A. Winnik, I. Manners, *Angew. Chem. Int. Ed.* 2005, **44**, 7964.
- G. R. Krishnan, Y. Yuan, A. Arzumand, D. Sarkar, *J. Polym. Sci. A*, 2014, **52**, 1917.
- X. Yu, Y. Li, D. Wu, Z. Ma and S. Xing, *New J. Chem.* 2013, **37**, 1201.
- J. Zou, F. Zhang, Y. Chen, J. E. Raymond, S. Zhang, J. Fan, J. Zhu, A. Li, K. Seetho, X. He, X. D. J. Pochan and K. L. Wooley, *Soft Matter*. 2013, **9**, 5951.
- S. Basak, J. Nandaa and A. Banerjee, *J. Mater. Chem.* 2012, **22**, 11658.
- S. Mukherjee and B. Mukhopadhyay, *RSC Adv.* 2012, **2**, 2270.
- P. Xue, J. Sun, B. Yao, P. Gong, Z. Zhang, C. Qian, Y. Zhang and R. Lu, *Chem. Eur. J.* 2015, **21**, 4712.
- K. Sugiyasu, N. Fujita and S. Shinkai, *Angew. Chem. Int. Ed.* 2004, **43**, 1229.
- F. G. Gandolfo, A. Bot, and E. Flöter, *J. Am. Oil Chem. Soc.* 2004, **81**, 1.
- J. F. Toro-Vazquez, J. A. Morales-Rueda, E. Dibildox-Alvarado, M. Charo-Alonso, M. González-Chávez and M. M. Alonzo-Macias, *J. Am. Oil Chem. Soc.* 2007, **84**, 989.
- T. Laredo, S. Barbut and A. G. Marangoni, *Soft Matter*, 2011, **7**, 2734.
- A. K. Zetzl, A. G. Marangoni and S. Barbut, *Food Funct.* 2012, **3**, 327.
- M. A. Rogers, A. J. Wright and A. G. Marangoni, *Soft Matter*, 2008, **4**, 1483.
- A. Motulsky, M. Lafleur, A.-C. Couffin-Hoarau, D. Hoarau, F. Boury, J.-P. Benoit, J.-C. Leroux, *Biomaterials*, 2005, **26**, 6242.
- A.-C. Couffin-Hoarau, A. Motulsky, P. Delmas and J.-C. Leroux, *Pharm. Res.* 2004, **21**, 454.
- A. Vintiloiu, M. Lafleur, G. Bastiat, J.-C. Leroux, *Pharm Res.* 2008, **25**, pp. 845.
- L. Lukyanova, S. Franceschi-Messant, P. Vicendo, E. Perez, I. Rico-Lattes and R. Weinkamer, *Colloids Surf., B*, 2010, **79**, 105.
- K. Iwanaga, T. Sumizawa, M. Miyazaki, M. Kakemi, *Int. J. Pharm.*, 2010, **388**, 123.
- K. Iwanaga, M. Kawai, M. Miyazaki and M. Kakemi, *Int. J. Pharm.*, 2012, **436**, 869.
- (a) P. D. Thornton, S. M. R. Billah and N. R. Cameron, *Macromol. Rapid Commun.* **34**, 257; (b) P. D. Thornton and A. Heise, *Chem. Commun.* 2011, **47**, 3108.
- (a) M. Khuphe, A. Kazlauciuonas, M. Huscroft and P. D. Thornton, *Chem. Commun.* 2015, **51**, 1520; (b) S. Hehir and N. R. Cameron, *Polym. Int.* 2014, **63**, 943; (c) G. J. M. Habraken, A. Heise and P. D. Thornton, *Macromol. Rapid Commun.* 2012, **33**, 272.
- P. D. Thornton, R. Brannigan, J. Podporska, B. Quilty and A. Heise, *J. Mater. Sci: Mater. Med.* 2012 **23**, 37.
- (a) M. I. Gibson and N. R. Cameron, *Angew. Chem. Int. Ed.* 2008, **47**, 5160; (b) C. Bonduelle and S. Lecommandoux, *Biomacromolecules*, 2013, **14**, 2973.
- S. Manchun, C. R. Dass, P. Sriamornsak, *Life Sciences.* 2012, **90**, 381.
- G. J. M. Habraken, C. E. Koning and A. Heise, *J. Polym. Sci. A Polym. Chem.* 2009, **47**, 6883.
- M. Rogers, A. Smith, A. Wright and A. Marangoni, *J. Am. Oil Chem. Soc.* 2007, **84**, 899.
- A. Pal, Y. K. Ghosh and S. Bhattacharya, *Tetrahedron*, 2007, **63**, 7334.
- K. J. Skilling, F. Citossi, T. D. Bradshaw, M. Ashford, B. Kellam and M. Marlow, *Soft Matter*, 2014, **10**, 237.
- P. Bairi, B. Roy, P. Routh, K. Sen and A. K. Nandi, *Soft Matter*, 2012, **8**, 7436.
- C. Daniel, C. Dammer and J.-M. Guenet, *Polymer*, 1994, **35**, 4243.
- A. Lejardi, R. Hernández, M. Criado, J. I. Santos, A. Etxeberria, J. R. Sarasua and C. Mijangos, *Carbohydr. Poly.* 2014, **103**, 267.

- 41 J. Fan, J. Zou, X. He, F. Zhang, S. Zhang, J. E. Raymond and K. L. Wooley, *Chem. Sci.*, 2014, **5**, 141.
- 42 M. Guardigli, A. Lundin and A. Roda, *Chemiluminescence and Bioluminescence: Past, Present and Future*. The Royal Society of Chemistry, 2011, 141.
- 43 (a) C. de Duve, T. de Barsy, B. Poole, A. Trouet, P. Tulkens, F. Van Hoof, *Biochem Pharmacol*, 1974, **23**, 2495. (b) N. Fehrenbacher and M. Jättelä, *Cancer Res.* 2005, **65**, 2993.
- 44 (a) R. Haag and F. Kratz, *Angew. Chem. Int. Ed.* 2006, **45**, 1198. (b) H. R. Krüger, G. Nagel, S. Wedepohla and M. Calderón, *Nanoscale*, 2015, **7**, 3838. (c) B. Cortese, S. D'Amone, G. Gigli and I. E. Palamà, *Med. Chem. Commun.* 2015, **6**, 212. (d) I. E. Palamà, B. Cortese, S. D'Amone, V. Arcadio and G. Gigli, *Biomater. Sci.* 2015, **3**, 361. (e) A. Hakeem, R. Duan, F. Zahid, C. Dong, B. Wang, F. Hong, X. Ou, Y. Jia, X. Lou and F. Xia, *Chem. Commun.* 2014, **50**, 13268.
- 45 D. Ramyadevi and K. S. Rajan, *RSC Adv.* 2015, **5**, 12956.
- 46 H. Wu, B.-B. Ni, C. Wang, F. Zhai and Y. Ma, *Soft Matter*, 2012, **8**, 5486.
- 47 H. Bunzen and E. Kolehmainen, *Molecules*, 2013, **18**, 3745.
- 48 R. W. Korsmeyer, R. Gurny, E. M. Doelker, P. Buri and N.A. Peppas, *Int. J. Pharm.* 1983, **15**, 25.